ACS OMEGA

http://pubs.acs.org/journal/acsodf

Article

Experimental Study of the Pore Structure and Gas Desorption Characteristics of a Low-Rank Coal: Impact of Moisture

Mingyi Chen,* Xiaoyun Chen, Xuejie Zhang, Fuchao Tian, Weili Sun, Yumeng Yang, and Tonghao Zhang

Cite This: *ACS Omega* 2022, 7, 37293−37303

Read Online

ACCESS | Metrics & More | Article Recommendations

ABSTRACT: Coal−water interactions have a prominent impact on the prediction of coal mine gas disasters and coalbed methane extraction. The change of characteristics in the microscopic pores of coal caused by the existence of water is an important factor affecting the diffusion and migration of gas in coal. The low-pressure nitrogen adsorption experiments and gas desorption experiments of a low-rank coal with different equilibrium moisture contents were conducted. The results show that both the specific surface area and pore volume decrease significantly as the moisture content increases, and the micropores (pore diameter <10 nm) are most affected by the water adsorbed by coal. In particular, for a water-equilibrated coal sample at 98% relative humidity, micropores with pore sizes smaller than 4 nm as determined by the density functional theory model almost disappear, probably due to the blocking effects of water clusters and capillary water. In this case, micropores with a diameter less than 10 nm still contribute most of the specific surface area for gas adsorption in coal. Furthermore, the fractal dimensions at relative pressures of 0−0.5 (D_1) and 0.5−1 (D_2) calculated by the Frenkel−Halsey−Hill model indicate that when the moisture content is less than 4.74%, D_1 decreases rapidly, whereas D_2 shows a slight reduction as the moisture content increased. In contrast, when the moisture content exceeds 4.74%, further increases in the moisture content cause D_2 to decrease significantly, while there is nearly no change for D_1. The correlation analyses show that the ultimate desorption volume and initial desorption rate are closely related to the fractal dimension D_1, while the desorption constant (K_t) mainly depends on the fractal dimension D_2. Therefore, the gas desorption performances of coal have a close association with the pore properties of coal under water-containing conditions, which indicate that the fluctuation in moisture content should be carefully considered in the evaluation of gas diffusion and migration performances of in situ coal seams.

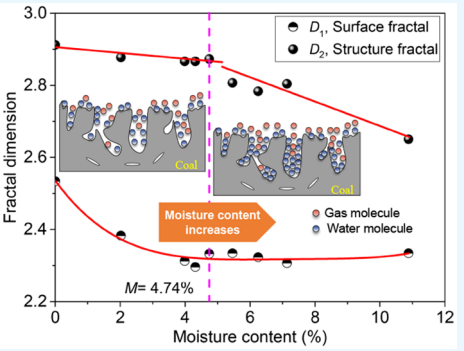

1. INTRODUCTION

Water is an inherent component of coal. The coal−water interactions have a significant influence on coalbed methane (CBM) extraction, coal utilization, and the prediction of coal mine gas disasters.[1−3] In the CBM field, the inherent moisture of coal is considered to be an important factor that affects the interactions between coal and gas.[4] The inherent moisture is mainly absorbed on the surface sites of coal pores due to the physical adsorption and the effects of oxygen-containing functional groups.[5] Moreover, the existing oxygen-containing functional groups are preferentially occupied by the adsorbed water molecules.[6] Through long-term research, researchers have found that the existence of water can diminish gas (e.g., CH_4, CO_2) adsorption, diffusion, and seepage capacities of coal.[7,8] Based on this, to effectively control gas disasters or improve the CBM recovery rate, a variety of technologies have been proposed to regulate the coal−water interactions of in situ coal seams.[9−11] Unfortunately, the fundamental understanding of the pore characteristics of coal-containing water and the relations with gas occurrence and migration capacities are still unclear.

Many scholars have long been concerned about the influence of moisture on gas adsorption and desorption properties of coal through experimental, numerical simulation, and mathematical theoretical methods. The presence of water can significantly reduce the methane adsorption capacity of coal,[12,13] which is mainly due to the competitive adsorption by water and methane and the advantageous adsorption of water by coal.[14,15] It has been reported that a 2% moisture content can result in the reductions of approximately 20% for both the CH_4 and CO_2 adsorption capacities of moist coal.[16] The impact of water on the gas adsorption capacity of coal is also

Received: June 18, 2022
Accepted: October 4, 2022
Published: October 14, 2022

https://doi.org/10.1021/acsomega.2c03805
ACS Omega 2022, 7, 37293−37303

related to the degree of metamorphism coal seams have suffered. Dry coal shows a trend for methane adsorption capacity that first falls and then rises with increasing coal rank, whereas the methane adsorption capacity of water-equilibrated coal increases slightly with coal rank.[17] It was further found that the adsorbed water induces reductions in the methane adsorption capacity of bituminous coal, and that non-adsorbed water has no effect; in contrast, for anthracite coal, both forms of water remarkably diminish methane adsorption, which is considered to be related to the difference in pore structures for the two coal samples.[18] In addition, increasing the moisture content can decrease the desorption volume and desorption velocity of methane gas in coal, which has been widely accepted by scholars.[19,20] Moreover, the existence of water has a high negative impact on the methane diffusion capacity of coal.[4,21] Combined with the unipore, bidisperse, and other diffusion models, it was observed that increasing moisture content caused both micropore and macropore diffusion coefficients to decrease for coals with different ranks.[22,23] Other studies further show that increasing the equilibrium moisture content induces a continual decrease in diffusivity for anthracite coal and a U-shaped change in diffusivity for bituminous coal. This is considered to be caused by different moisture effects resulting in the reductions in the adsorbed gas volume and the decreases in pore space for various coals.[24]

Generally, coal with $R_{o,max}$ less than 0.65% is classified as low-rank coal in China,[25] and this includes lignite and some long-flame coal. Low-rank coal generally features an adsorbed water content higher than that of middle-rank coal and high-rank coal because low-rank coal has considerable porosity and more oxygen-containing functional groups.[2,7] Statistics show that the moisture content of lignite in China is 10−28%, and that of long-flame coal is mostly 3−12%.[26] In this study, long-flame coal from Baoji city in China was used to study (1) the water adsorption behavior of coal and the pore structure of water-equilibrated coals with different moisture contents using the low-pressure nitrogen gas adsorption (LN_2GA) method, (2) the relationships between the adsorbed moisture content and the fractal dimensions of coal pores, and (3) the impact of the adsorbed moisture on the methane desorption performance of coal and its relations with fractal dimensions. In this paper, the research on the influences of the adsorbed moisture on the pore characteristics of coal is the main innovation. This study will be helpful to understand the relationships between coal pores and gas storage and migration performances of coal under the influence of water.

2. EXPERIMENTS AND METHODS

2.1. Coal Preparation and Basic Parameters.

2.1.1. Basic Parameters. The low-rank coal sample was selected from the No. 2 coal seam in the Yuanzigou coal mine, Baoji city, Shaanxi Province. Geological survey data show that the moisture content of the No. 2 coal seam on an air-dry basis ranges between 3.60−11.28%. Several kilograms of fresh lump coal were collected from the working face, and various sizes of coal particles were prepared by crushing and screening. Following the ISO 17246:2010 standard, a coal sample with a particle size of 80−200 mesh was selected to perform the proximate analysis by an automatic proximate analyzer (5E-MAG6600). The vitrinite reflectance of coal reflects the coalification degree, which was determined by following the ISO 7404−5:2009 standard. The moisture content on an air-dry basis (M_{ad}), ash content on an air-dry basis (A_{ad}), volatile matter on a dry ash free basis (V_{daf}), fixed carbon on an air-dry basis (FC_{ad}), and maximum vitrinite reflectance ($R_{o,max}$) are shown in Table 1.

Table 1. Basic Parameters for the Coal Sample

sample	$R_{o,max}$ (%)	M_{ad} (%)	A_{ad} (%)	V_{daf} (%)	FC_{ad} (%)
long-flame coal	0.65	6.33	26.59	40.53	39.90

2.1.2. Preparation of Moist Coal Samples. First, a certain amount of pulverized coal with a particle size of 60−80 mesh was placed in a vacuum drying oven at 378 K for at least 8 h to remove the original moisture. Eight saturated salt solutions were selected to prepare water-equilibrated coal samples under constant relative humidity (RH) conditions. The RH was 11% for LiCl, 23% for CH_3COOK, 33% for $MgCl_2$, 43% for K_2CO_3, 57% for NaBr, 75% for NaCl, 85% for KCl, and 98% for K_2SO_4 at a room temperature of 293 K. Approximately 5 g of coal sample was placed in glassware containing a saturated salt solution, and the glassware was sealed with vacuum silica gel. A high-precision electronic balance (FA2204) was used to weigh the coal samples at 8 h intervals. When the weight of the sample remained steady, it was considered that water adsorption equilibrium was achieved under the corresponding RH conditions. Subsequently, the moisture content of the coal sample under different RH conditions was calculated using the following equation:

$$M = \frac{(m_{moist} - m_{dry})}{m_{dry}} \quad (1)$$

where M is the moisture content, %; m_{moist} is the weight of the moist sample at a certain RH, g; and m_{dry} is the weight of the dry sample, g. The water adsorption test at each RH value was repeated twice, and the mean value of moisture contents was determined for further study.

Furthermore, the water adsorption characteristics of the studied coal were analyzed with a modified Guggenheim−Anderson−de Boer (M-GAB) model. The M-GAB model is based on the BET and GAB models and has been proven to offer good characterization of water vapor adsorption on porous materials.[27] The M-GAB model, similar to the GAB and M-Dent models,[28] assumes water molecules adsorb on two sites: primary adsorption sites and secondary adsorption sites, and one molecule occupies α sites during adsorption. The M-GAB model can be described by the following equation:

$$M = \frac{M_0 CKx^{\alpha}}{(1 - Kx^{\alpha})(1 - Kx^{\alpha} + CKx^{\alpha})} \quad (2)$$

where M_0 is the monolayer adsorption capacity, x is the relative humidity, C and K are the adsorption constants related to primary sites and secondary sites, respectively, and α represents the heterogeneity of the adsorption system. The amounts of water adsorbed on primary and secondary sites have the following relationships:[29]

$$M_1 = \frac{M_0(C - 1) \times Kx^{\alpha}}{1 - Kx^{\alpha} + CKx^{\alpha}} \quad (3)$$

$$M_2 = \frac{M_0 Kx^{\alpha}}{1 - Kx^{\alpha}} \quad (4)$$

2.2. Low-Pressure Nitrogen Gas Adsorption Test.

Low-pressure nitrogen gas adsorption (LN_2GA) is an

https://doi.org/10.1021/acsomega.2c03805
ACS Omega 2022, 7, 37293−37303

important physical method used to characterize nanopores in porous media. In this study, the test instrument was an Autosorb-iQ2 analyzer (Quantachrome Ins, USA). The N_2 ad/desorption isotherms for coal samples were measured with P/P_0 values of 0.001−0.995. Before the LN_2GA tests and according to the moist coal preparation processes described in section 2.1.2, the coal samples with different water contents were prepared. Then the moist coal samples were placed in a liquid N_2 environment at a temperature of ∼77 K for several minutes. Under these conditions, the moist samples were frozen so that the loss of preadsorbed water could be ignored. Moreover, the vacuum pumping step was omitted to avoid the loss of water from the tested samples.

2.3. Tests and Analytical Methods for Methane Desorption in Coal. *2.3.1. Methane Desorption Tests.* The bulk desorption method[30] was applied to perform methane desorption tests for coal samples with particle sizes of 60−80 mesh. First, approximately 50 g of coal sample was placed in a coal sample tank. To reduce the loss of water from the coal sample as much as possible, the vacuum pumping time was no longer than 30 min. Then methane gas with a purity of 99.99% was pumped into the coal sample tank to establish a gas pressure, and the coal sample tank was placed in a stable temperature water bath at 303.15 K. Subsequently, the gas pressure of the coal sample tank was adjusted to a predetermined pressure (1 MPa). When the pressure gauge remained constant for 8 h, it was deemed that the gas-containing coal sample had achieved adsorption equilibrium. Finally, the free gas of the coal sample tank was removed, and then a methane desorption test was performed on the coal. The test time was 120 min, and the methane desorption volume and the ultimate desorption volume (Q_∞) were recorded at regular intervals. The moisture contents of the test samples were measured by the weighing method after the methane desorption tests.

2.3.2. Analytical Methods for Desorption Data. Numerous mathematical equations have been proposed to describe gas desorption laws for coal particles.[31] Among them, the Airey-type and Winter-type equations are often used to analyze the laws for understanding coal seam gas desorption and emission.

Airey believed that the coal body could be regarded as a material composed of separated blocks containing fractures and proposed the following formula:[32]

$$Q_t = A\left[1 - \exp\left\{-\left(\frac{t}{t_0}\right)^n\right\}\right] \quad (5)$$

where Q_t is the gas desorption volume at time t, cm^3/g; A is the ultimate desorption volume, cm^3/g; t_0 is the desorption time constant; and n is a coefficient.

In Winter's theory, when the gas pressure is removed, the change in the gas desorption rate with time can be explained by a power formula.[33] Furthermore, after mathematical integration of the established power equation, the relationship between gas desorption volume and time is proposed and can be described by the following equation, namely, the Winter-type equation:[31,34]

$$Q_t = \frac{V_1}{1 - K_t} t^{1-K_t} \quad (6)$$

where Q_t is the cumulative desorption volume at time t, cm^3/g; V_1 is the initial desorption rate of gas desorption at time t_1, $cm^3/(g\cdot min)$; and k_t is a constant that reflects the degree of attenuation of the desorption rate.[35]

3. EXPERIMENTAL RESULTS

3.1. Water Adsorption Isotherms. The fitting of water adsorption data from a studied coal sample with the M-GAB model is shown in Figure 1. According to the International Union of Pure and Applied Chemistry (IUPAC) classification,[36] the adsorption curve is a type II isotherm. The M-GAB model has an excellent fit with an R^2 value of 0.9975. Under the conditions of RH < 0.2 and RH > 0.8, the amount of adsorbed water increases rapidly. When the RH ranged from 0.2 to 0.8, the growth in the water adsorption capacity is relatively slow.

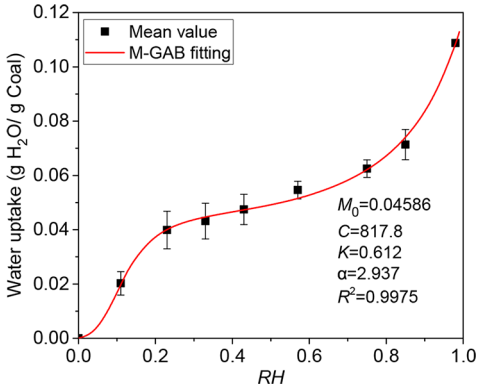

Figure 1. M-GAB model fitting for water adsorption by the studied sample.

3.2. LN_2GA Isotherms. The LN_2GA adsorption and desorption isotherms of the coal samples are illustrated in Figure 2. The adsorption isotherms for dry and moist samples are classified as type II according to the IUPAC classification. As the moisture content increases, the slopes of the nitrogen adsorption curves decrease in the pressure range of 0.1 to 0.9. The maximum amount of nitrogen adsorbed by the dry coal sample is 20.24 cm^3/g, whereas that of the water-equilibrated coal sample at 98% RH (M = 10.88%) is reduced by nearly 50%. In the low relative pressure range (P/P_0 < 0.01), the nitrogen adsorption capacities of coal samples generally increase significantly, which is mainly related to the micropore filling effect caused by the large number of micropores in coal.[37,38] In particular, the nitrogen adsorption curves become flatter at P/P_0 < 0.1 with increasing moisture content, which indicate that the micropore filling effect is weakened for gas adsorption on moist coal samples.

Moreover, all coal samples show prominent adsorption hysteresis. The features of the hysteresis loops of coal samples correspond to types H3 and H4 according to the IUPAC classification,[39] and the sizes of the hysteresis loops of coal samples decrease with increasing moisture content. The coal samples with moisture contents less than 7.14% (corresponding to an RH of 85%) exhibit an inflection point in the desorption curve at a P/P_0 value of approximately 0.45, which is thought to be related to the presence of ink-bottle pores.[40,41] The desorption curves near the inflection point shrink as the moisture content increases. When the moisture content increases to the maximum equilibrium moisture content (10.88%), the inflection point of the desorption curve almost disappears.

https://doi.org/10.1021/acsomega.2c03805
ACS Omega 2022, 7, 37293−37303

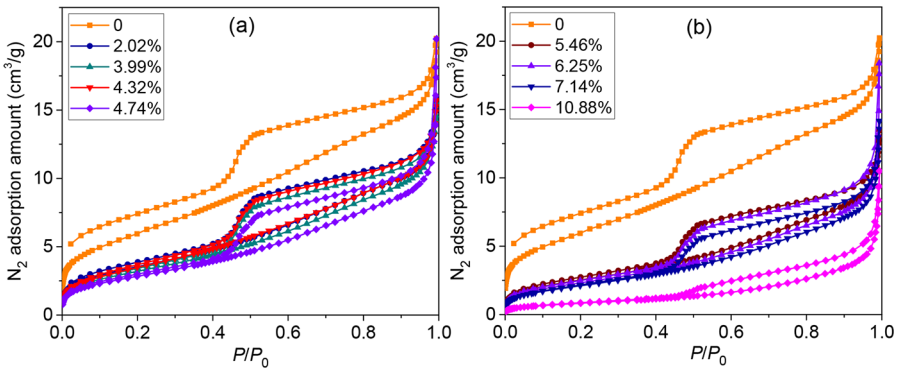

Figure 2. Low-pressure nitrogen ad/desorption isotherms of coal samples with different moisture contents: (a) moisture contents of 0−4.74% and (b) moisture contents of 5.46−10.88%.

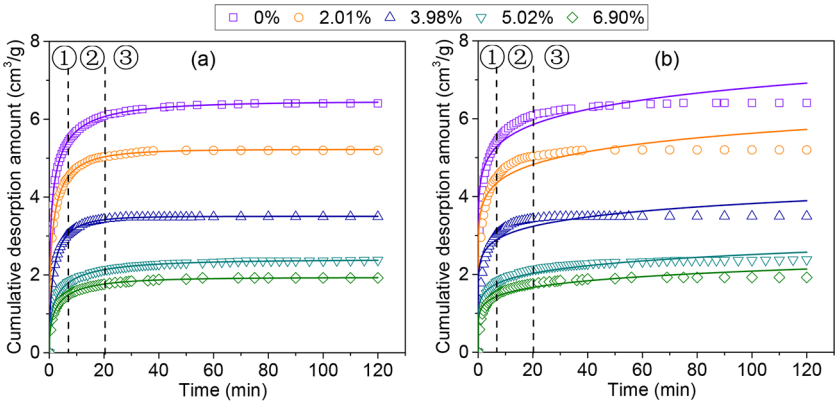

Figure 3. Methane desorption data and fitting curves determined for coal samples with different moisture contents at a methane pressure of 1 MPa: (a) Airey-type fit and (b) Winter-type fit.

Table 2. Fitting Results for the Tested Samples with the Airey-Type and Winter-Type Equations

	Airey's equation				Winter's equation		
moisture content (%)	A (cm^3/g)	t_0 (min)	n	R^2	V_1(cm^3/(g·min))	k_t	R^2
0	6.460	1.406	0.387	0.9998	0.413	0.907	0.9373
2.01	5.225	1.530	0.463	0.9997	0.347	0.904	0.9013
3.98	3.504	1.901	0.554	0.9997	0.245	0.897	0.8670
5.02	2.392	3.329	0.446	0.9989	0.180	0.868	0.9290
6.90	1.934	3.175	0.484	0.9989	0.153	0.861	0.9139

Table 3. Methane Desorption Amounts for Different Desorption Periods

moisture content (%)	Q_1 (cm^3/g)	Q_{3-5} (cm^3/g)	Q_∞ (cm^3/g)	$\left\|\frac{A-Q_\infty}{Q_\infty}\right\|$ (%)
0	3.791	0.413	6.406	0.85
2.01	2.950	0.405	5.199	0.50
3.98	1.778	0.325	3.496	0.22
5.02	1.018	0.177	2.380	0.54
6.90	0.857	0.172	1.922	0.63

3.3. Methane Desorption Characteristics. The fitting curves of the Winter-type and Airey-type equations are shown in Figure 3 for methane desorption isotherms determined at a gas pressure of 1 MPa. The desorption process can be divided into a rapid growth period (①), stable growth period (②) and slow growth period (③). The cumulative desorption amounts show monotonous upward parabolic trends with increasing desorption time. In addition, the cumulative desorption amounts of the coal samples decrease as the moisture content increases.

The fitting results for the Airey-type and Winter-type equations are shown in Table 2. The correlation coefficients R^2 for the Airey-type equation were 0.9989−0.9998; for the Winter-type equation, the values were 0.8670−0.9373. Apparently, the Airey-type equation exhibits a higher fit accuracy than the Winter-type equation. Moreover, the parameters A and V_1 represent the ultimate methane desorption capacity and the initial rate of methane desorption, respectively.[22,34] A significant reduction in the methane

https://doi.org/10.1021/acsomega.2c03805
ACS Omega 2022, 7, 37293−37303

desorption capacity can be observed with the increases of moisture content.

Furthermore, the amounts of methane desorbed at different periods are illustrated in Table 3. The volumes of methane desorbed from coal in the first minute (Q_1) and during the third to fifth minutes (Q_{3-5}) are two important parameters used for predicting the risk of coal and gas outburst of a coal seam.[31] The errors of parameter A are 0.22−0.85% for a methane pressure of 1 MPa, and thus, parameter A is very close to the measured value Q_∞. Therefore, the Airey-type equation is more suitable for describing the methane desorption behavior of coal.

4. ANALYSIS AND DISCUSSION

4.1. Water Adsorption Behavior of Coal. The water adsorption isotherms calculated for primary sites and secondary sites by the M-GAB model are plotted in Figure 4

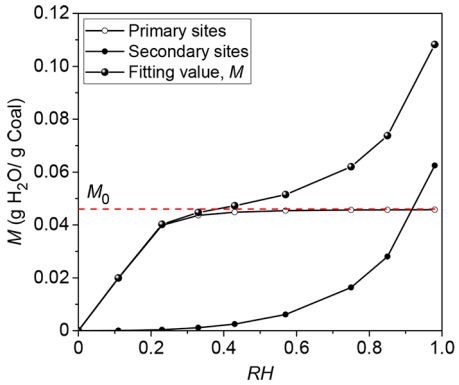

Figure 4. Amounts of water adsorbed on primary sites and secondary sites.

for the studied coal samples. The initial amount of water adsorbed is mainly contributed by primary sites, and the primary site adsorption isotherms coincided with type I behavior according to the IUPAC classification,[36] which signifies that primary site adsorption is confined to a monolayer. With the increase in relative humidity, the secondary site adsorption becomes crucial, and the secondary site adsorption corresponds to type III isotherms associated with multilayer adsorption. An inflection point at a RH of approximately 0.2 can be observed in the M-GAB fitting curve, indicating the completion of monolayer coverage and the beginning of multilayer adsorption.[39] When the RH exceeds 0.5, the primary adsorption approached the dotted line representing the monolayer adsorption capacity (M_0) calculated by the M-GAB model, and then water clusters gradually form.[42] As the RH increases, the water uptake increases sharply in the region RH > 0.8, which is related to the capillary condensation of water in coal pores.

In the M-GAB model, C is related to the adsorption energies of water molecules on primary sites, while K is associated with the adsorption energies for interactions between water molecules and adsorbed water molecules on the secondary sites.[27,28] For the studied coal sample, the value of C is far larger than that of K, which is mainly because the weak interactions between coal and water molecules required more energy than the strong water−water interactions.[28,42]

4.2. Impact of Water on the Pore Structure of Coal. *4.2.1. N_2-SSA and N_2-PV.* The pore size classification method proposed by B.B. Hodot has been widely used, and coal pores can be divided into five categories.[43,44] Among them, micropores (d < 10 nm) constitute the gas adsorption volume of coal, transition pores (10<d < 100 nm) are the gas diffusion spaces, the pore diameter of 100 nm is always considered to be a cutoff point for gas diffusion and seepage,[34] and mesopores (100<d < 1000 nm) form a slow seepage space. In this paper, after integrating the pore parameters from the density functional theory (DFT) model (1−10 nm) and the Barrett−Joyner−Halenda (BJH) model (10−300 nm), the specific surface area (SSA) and pore volume (PV) are calculated for different pore scales (micropores, transition pores, and mesopores), as illustrated in Table 4. When the moisture content increases to an equilibrium moisture content of 2.02% (corresponding to an RH of 11%), the total SSA is decreased by approximately 39.3%. With increasing moisture content, both the total SSA and total PV tend to decrease, whereas the average pore diameter (PD) shows a tendency to increase. For the water-equilibrated coal sample at 98% RH (M = 10.88%), the total SSA and total PV are reduced to 16.31 and 53.47%, respectively. This indicates that the adsorbed water leads to significant reductions in the SSA and PV.

The percentages of SSA and PV for different scale pores (micropores, transition pores, and mesopores) are shown in Figure 5. The micropore SSA for sample YZG1 accounts for 93.11% of the total SSA, which indicates that micropores play a key role in gas adsorption under dry conditions. The percentage of micropores SSA shows a decreasing trend with increasing moisture content, and that of sample YZG9 decreases to the lowest value (67.71%). This indicates that the micropores still contribute most sites for nitrogen

Table 4. Pore Parameters for Coal Samples from LN_2GA Tests[a]

		SSA (m^2/g)				PV ($\times10^{-3}$ cm^3/g)				
sample no.	mean moisture content (%)	S1	S2	S3	total	V1	V2	V3	total	PD (nm)
YZG1	0	16.44	1.12	0.096	17.66	18.79	7.20	4.83	30.82	5.66
YZG2	2.02	9.59	1.02	0.101	10.71	12.52	6.86	4.91	24.28	7.51
YZG3	3.99	8.72	1.03	0.096	9.85	11.75	6.98	5.09	23.82	7.97
YZG4	4.32	9.47	1.01	0.098	10.57	12.52	6.76	4.84	24.12	7.29
YZG5	4.74	7.68	1.01	0.24	8.93	10.53	7.26	13.50	31.29	11.63
YZG6	5.46	6.80	0.96	0.094	7.85	9.55	6.50	4.74	20.79	8.88
YZG7	6.25	6.23	0.99	0.21	7.43	8.91	7.33	10.98	27.23	12.38
YZG8	7.14	5.65	0.96	0.13	6.73	8.20	6.84	6.80	21.84	10.81
YZG9	10.88	1.95	0.79	0.14	2.87	3.35	5.94	7.19	16.48	20.50

[a]Note: Si and Vi represents the SSA and PV of micropores, transition pores and mesopores, respectively, where i = 1, 2, 3.

https://doi.org/10.1021/acsomega.2c03805
ACS Omega 2022, 7, 37293−37303

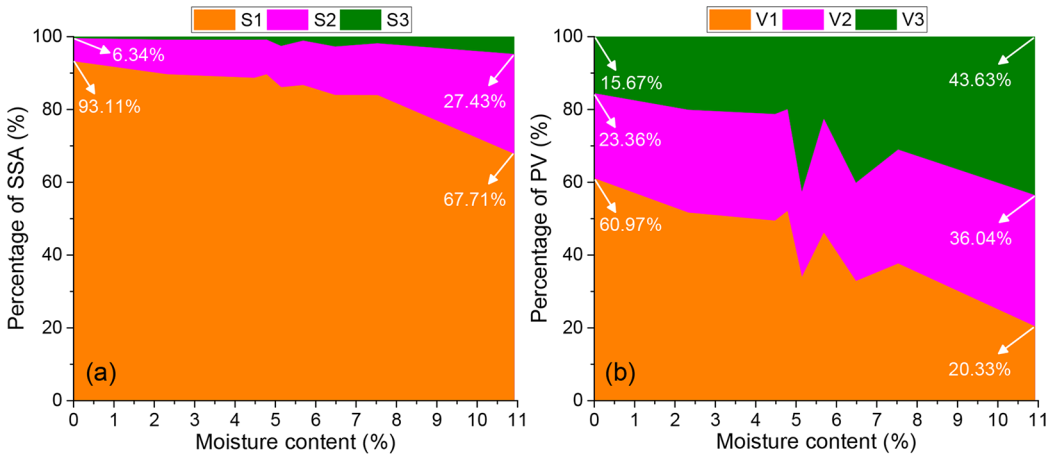

Figure 5. Changes in the percentages of SSA and PV for different scale pores with the moisture content: (a) percentage of SSA and (b) percentage of PV.

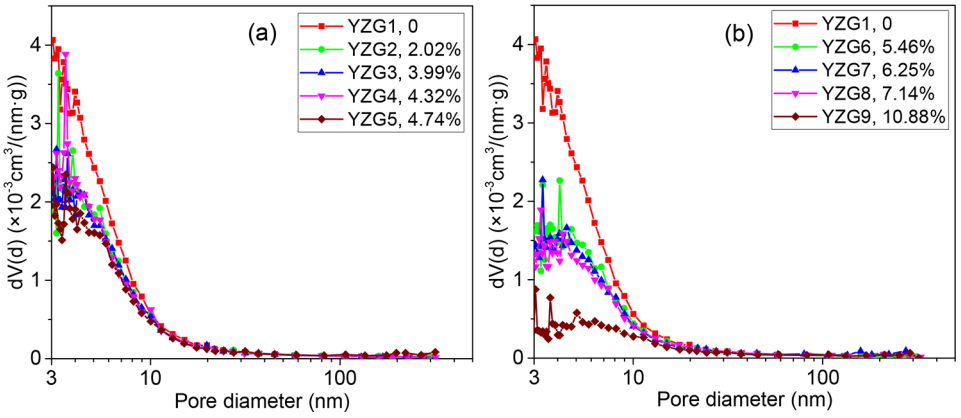

Figure 6. BJH-PSD curves for coal samples: (a) moisture contents of 0−4.74% and (b) moisture contents of 5.46−10.88%.

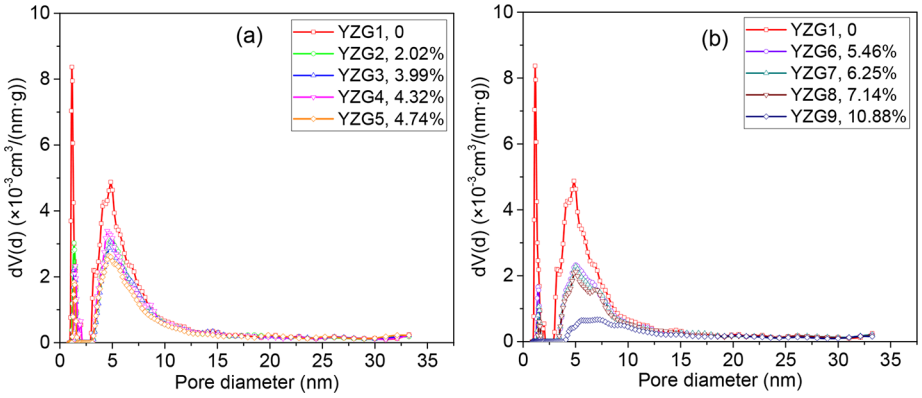

Figure 7. DFT-PSD curves for coal samples: (a) moisture contents of 0−4.74% and (b) moisture contents of 5.46−10.88%.

adsorption on water-equilibrated coal even under the maximum relative humidity condition. With increasing moisture content, the percentage of micropores volume also shows a decreasing trend. What's more, the percentage of micropores volume is 60.97% for sample YZG1 under dry conditions and only 20.33% for sample YZG9 under water-equilibrated conditions with 98% RH. In contrast, the percentages of SSA and PV of both transition pores and mesopores show the increasing trends. Therefore, the preadsorbed water significantly reduces the SSA and PV of coal pores. In particular, the micropores (d < 10 nm) are most significantly diminished by the presence of water.

4.2.2. Pore Size Distribution. Thommes et al.[39] indicated that the BJH method is more suitable for pore size analyses of mesopores and larger pores (>10 nm), and the DFT method provides a reasonably reliable assessment of nanopore size distributions. In this study, both DFT and BJH models are employed to investigate the PSDs (pore size distributions) of pores with sizes of 1−300 nm. The BJH-PSD curves for the coal samples are illustrated in Figure 6. All samples show multipeak distribution characteristics, and there were large

https://doi.org/10.1021/acsomega.2c03805
ACS Omega 2022, 7, 37293−37303

Table 5. Fractal Dimensions Calculated by the FHH Model for Low-Pressure Nitrogen Desorption Isotherms

sample no.	mean moisture content (%)	A_1	$D_1 = 3 + A_1$	$D_1 = 3 + 3A_1$	R^2	A_2	$D_2 = 3 + A_2$	$D_2 = 3 + 3A_2$	R^2
YZG1	0	−0.466	2.534	1.602	0.9533	−0.088	2.912	2.737	0.9769
YZG2	2.02	−0.617	2.383	1.149	0.9594	−0.123	2.877	2.632	0.9604
YZG3	3.99	−0.687	2.313	0.938	0.9543	−0.134	2.866	2.599	0.9695
YZG4	4.32	−0.704	2.296	0.888	0.9649	−0.127	2.873	2.619	0.9737
YZG5	4.74	−0.667	2.333	0.998	0.9605	−0.193	2.807	2.421	0.9586
YZG6	5.46	−0.666	2.335	1.004	0.9561	−0.147	2.853	2.558	0.9575
YZG7	6.25	−0.677	2.323	0.970	0.9629	−0.216	2.784	2.351	0.9638
YZG8	7.14	−0.694	2.306	0.919	0.9826	−0.196	2.804	2.412	0.9471
YZG9	10.88	−0.666	2.334	1.003	0.9914	−0.349	2.651	1.952	0.9360

numbers of nanopores in the size range of 3−300 nm. With increasing moisture content, the dV(d) values of coal samples gradually approach the *X*-axis, especially for micropores (d < 10 nm). The DFT-PSD curves for the coal samples are shown in Figure 7. The DFT $dV(d)$ plots for coal samples with moisture contents less than 7.14% mainly exhibit two peak values at ∼1.1 nm and ∼5.0 nm, whereas that of sample YZG9 (M = 10.88%) shows a single peak at ∼5.6 nm. The DFT dV(d) value tends to decrease with increasing moisture content, and when the moisture content reaches 10.88%, the peak value of dV(d) approaches 0 at ∼1.1 nm, thereby indicating that pores less than 4 nm almost disappear for water-equilibrated coal sample YZG9. For both the DFT-PSD and BJH-PSD curves, there is no significant difference in the PSDs for pores greater than 10 nm in coal samples with different moisture contents.

Therefore, the preadsorbed water mainly influences the micropores (d < 10 nm) of coal, which can be attributed to the adsorption of water on the coal surface. With a low moisture content, the effective adsorption sites for CH_4 or N_2 molecules are decreased by the preferential adsorption of water molecules.[14,45] With a further increase in moisture content, multilayer adsorption occurs, and the thickness of the water molecule layer becomes significant. The process can result in the formation of water clusters.[42,46] Furthermore, the growth of water clusters and capillary condensation fills some small pores. With a further increase in the RH, the adsorbed moisture content of coal is enhanced (Figure 1). Especially for the water-equilibrated coal sample YZG9 at 98% RH, some pore throats can be blocked by the preadsorbed water, which hinder the intrusion of gas molecules into the micropores. Thus, the nanopores available for methane adsorption by water-equilibrated coal at 98% RH are mainly larger-scale pores (pore diameters >4 nm).

4.3. Fractal Characteristics of Coal Pores under Moist Conditions. Using the LN_2GA data, the fractal dimension can be determined by the fractal Frenkel−Halsey−Hill (FHH) equation,[47,48] which is described by the following expression:

$$\ln V = A\left[\ln \ln\left(\frac{P_0}{P}\right)\right] + B \tag{7}$$

where V is the amount of gas adsorbed at the adsorption equilibrium pressure P; P_0 is the saturated gas pressure; A is the slope of the fitting line, which is linear with the fractal dimension D, and there are two mathematical expressions for A and D, namely, $A = D - 3$ and $A = (D - 3)/3$; and B is a constant. The fractal dimension D ranges from 2 to 3 and reflects the irregularity of coal pores. The closer D is to 2, the smoother the pore surface; the closer D is to 3, the more complex the pore surface.

Low-pressure nitrogen desorption isotherms are generally used to calculate the fractal dimension because the corresponding adsorption state is more stable.[49] In the region with P/P_0 < 0.5, the adsorption and desorption curves are essentially parallel and even coincide, while in the region with P/P_0 > 0.5, there is significant adsorption hysteresis. This phenomenon suggests that the mechanisms for gas adsorption by coal are different for the two pressure regions. The fractal dimensions of the two regions are always calculated with a relative pressure of 0.5 as the dividing point.[50] The fractal dimensions D_1 and D_2 are for the low pressure range (0−0.5) and high pressure range (0.5−1), respectively. The fractal dimensions D calculated by the FHH equation are illustrated in Table 5. The results obtained with the equation $A = D - 3$ are between 2 and 3, which is more reasonable than the results from the equation $A = (D - 3)/3$. It can be seen that D_1 is 2.296−2.534 and D_2 is 2.651−2.912. The D_2 value is commonly higher than the D_1 value for each coal sample, which is consistent with many studies.[47,51,52] Hazra et al.[53] documented that the LN_2GA method is likely to provide unreliable estimates for pore characteristics of coal and organic-rich shale, mainly because of the lack of penetrability of nitrogen gas into fine pores within the organic matter. Consequently, the LN_2GA method may not be able to accurately reflect the fractal property of narrow micropores. However, this method should be competent for the fractal analysis of larger pores (e.g., mesopores and macropores). Many researchers have indicated that the capacity of gas adsorption on coal is closely related to the fractal dimension D_1 from the LN_2GA method, and the D_1 value can comprehensively characterize the impact of physical properties of coal, such as pore properties, on the gas adsorption capacity of coal.[49,50] To a certain extent, the surface fractal characteristics of coal pores can be represented by the fractal dimension D_1 from the LN_2GA method.

The relationships between the fractal dimensions D_1 and D_2 and the moisture content are shown in Figure 8. When the moisture content is less than 4.74% (corresponding to an RH of 43%), D_1 decreases rapidly, whereas D_2 decreases from 2.91 to 2.87, showing a slight change. When the moisture content increases from 4.74 to 10.88% (corresponding to an RH of 98%), D_2 decreases significantly, while D_1 remains at approximately 2.32.

Water sorption on coal is gradually divided into the following stages:[54] primary adsorption, secondary and multilayer adsorption, formation of water clusters, and capillary condensation of water. As illustrated in section 4.1, when the RH is lower than 43% (corresponding to an equilibrium moisture content of 4.74%), the adsorbed water content shows a Langmuir-type trend with increasing RH, indicating that

https://doi.org/10.1021/acsomega.2c03805
ACS Omega 2022, 7, 37293−37303

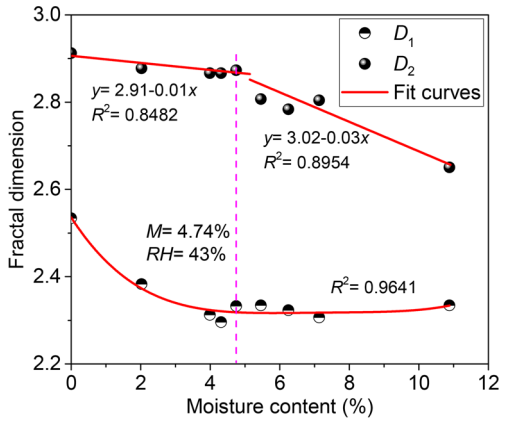

Figure 8. Relationships between fractal dimensions D_1 and D_2 and the moisture content.

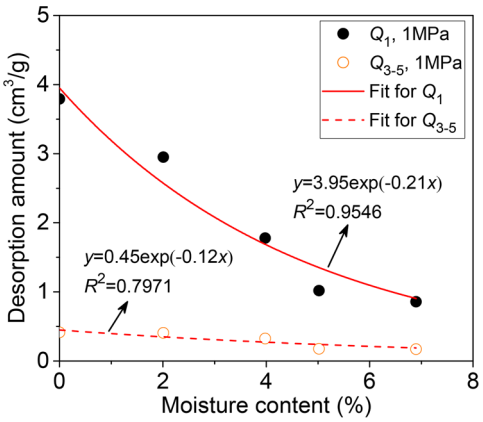

Figure 9. Relationships between Q_1, Q_{3-5}, and the moisture content.

water adsorption on coal mainly occurs at the primary sites, represented by oxygen-containing functional groups such as hydroxyl and carboxyl.[42,55] In this process, water molecules are preferentially adsorbed on the surfaces of micropores, which result in the enhanced homogeneity of micropore surfaces for water-equilibrated coal. This should be responsible for the significant reduction in fractal dimension D_1. As the relative humidity increases (RH > 43%), the secondary sites gradually become the main sites for adsorption. In this process, the formed water clusters grow continuously, and capillary condensation occurs. As shown in Figures 6 and 7, the PSD curves for micropores approach the X-axis, while those for larger-scale pores (pore diameter >10 nm) are basically unchanged. This shows that the water molecules adsorbed on the larger scale pores fail to cause significant variations in the nitrogen molecules adsorbed on the surfaces of larger scale pores. However, the formed water clusters and capillary water occupy the pore spaces and even fill some small pores and throats, thereby improving the homogeneity of the pore structure. These factors should be responsible for the reduction in fractal dimension D_2 (representing pore structure fractal dimension[49,50]) at the high moisture content stage (M > 4.74%). However, in the same stage, the fractal dimension D_1 is basically unchanged, which is mostly likely related to (i) the completion of saturated monolayer adsorption of water molecules on micropores and (ii) the inability of gas molecules to pass through some pores and throats blocked by the adsorbed water.

4.4. Impact of Moisture on Methane Desorption Performance. *4.4.1. Methane Desorption Characteristics of Moist Coals.* The gas desorption indices K_1 and Δh_2 are always selected as the methane desorption indices for the prediction of the outburst risks of mining coal seams.[31,56] The desorption index K_1 represents the amount of gas desorption within the first minute (Q_1), and the index Δh_2 is a gas desorption parameter expressed by the pressure differences of water column caused by the intrusion of the desorbed gas into a U-shaped instrument within the third to fifth minutes (Q_{3-5}).[31,44] The relationships between the initial desorption amounts Q_1 and Q_{3-5} and the moisture content are shown in Figure 9. The two desorption parameters decrease exponentially with the moisture content. In the range of moisture contents studied, the Q_1 and Q_{3-5} are reduced by 77.39 and 58.35%, respectively. Namely, each 1% increase in the moisture content led to an approximate 11% reduction in Q_1 and an approximate 8% reduction in Q_{3-5}. Therefore, moisture weakened the initial methane desorption capacity of coal, and Q_1 (corresponding to the K_1 index) is more significantly affected than Q_{3-5} (corresponding to the Δh_2 index).

As shown in Figure 10, the relationships between methane desorption parameters (V_1, A, K_t) and the moisture content are

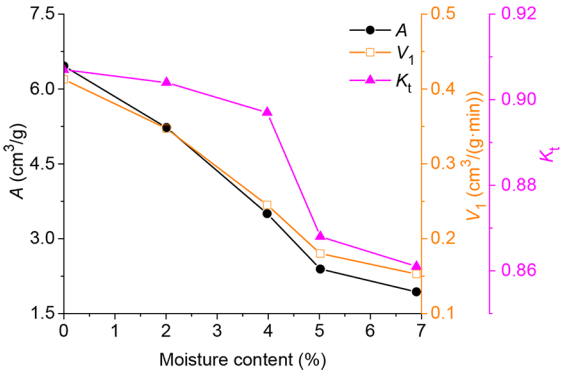

Figure 10. Changes in methane desorption parameters with the moisture content.

further studied with a methane pressure of 1 MPa. Below the studied moisture contents, the ultimate desorption amount (A) is decreased by approximately 0.66 cm³/g for each 1% increase in moisture content. For the initial desorption rate (V_1), each 1% increase in moisture content leads to a reduction of approximately 0.04 cm³/(g·min). Water molecules have more adsorption advantages than methane molecules and can prevent gas molecules from staying at some adsorption sites,[14,45] thereby reducing the saturated adsorption capacity of moist coal. Furthermore, the reduction in gas adsorption capacity decreases the concentration gradient for the desorbed gas and gas desorption amount,[57,58] which could cause the initial desorption rate of coal with low moisture content to be higher than that of coal with high moisture content. In addition, the desorption constant K_t shows a change trend different from those of parameters V_1 and A. When the moisture content is less than 3.98%, the parameter K_t decreases slightly, but it decreases significantly in the range 3.98−6.9%. As analyzed in section 4.3, it can be attributed to the fact that the constant K_t is mainly related to the fractal dimension D_2 representing the structural fractal characteristics of larger scale pores.

https://doi.org/10.1021/acsomega.2c03805
ACS Omega 2022, 7, 37293−37303

4.4.2. Relationship between the Fractal Dimensions and Desorption Parameters. Many researchers have indicated that the methane desorption performance of coal is related to the pore structure of coal under dry conditions.[34,59] In this study, the Pearson product−moment correlation coefficient (γ) was selected to further analyze this relationship under moist conditions. If the random variables $X = \{x_1, x_2, x_3, ..., x_n\}$, $Y = \{y_1, y_2, y_3, ..., y_n\}$, the Pearson correlation coefficient (γ) for the two variables is defined as

$$\gamma = \frac{n\sum x_i y_i - \sum x_i \sum y_i}{\sqrt{n\sum x_i^2 - (\sum x_i)^2}\sqrt{n\sum y_i^2 - \left(\sum y_i\right)^2}} \quad (8)$$

where n is the sequence length of the random variable, and γ ranges from −1 to +1. When γ is 0, the two variables are independent; when γ is [−1, 0], the two variables are negatively correlated, and when γ is [0, +1], the two variables are positively correlated. An absolute value of γ close to 1 suggests a high degree of correlation.

Using the interpolation method, the values of γ between methane desorption parameters (V_1, A, K_t) and fractal dimensions (D_1 and D_2) at a gas pressure of 1 MPa are calculated by SPSS software, as shown in Table 6. The values

Table 6. Correlation Coefficients between Fractal Dimensions and Desorption Parameters[a]

variables	A	V_1	K_t
D_1	0.854[a]	0.847[a]	0.684[a]
D_2	0.727[a]	0.729[a]	0.780[a]

[a]Significance level α = 0.01.

of γ for the correlations of A and D_1 or V_1 and D_1 are larger than 0.8, and these values are slightly higher than those for the correlations of A and D_2 or V_1 and D_2. Conversely, the value of γ for the correlation of D_2 and K_t is 0.780, which is greater than that for the correlation of D_1 and K_t. Therefore, the parameters A and V_1 are more closely related to the fractal dimension D_1, whereas the desorption constant K_t is more dependent on the fractal dimension D_2. This is mainly because the fractal dimensions D_1 and D_2 represent the surface fractal characteristics of micropores and the structural fractal characteristics of larger-scale pores, respectively.[49,50]

The methane desorption parameters A and V_1 reflect the ultimate and initial methane desorption capacities, which depend on the amount of methane adsorbed by the coal.[57] The micropores of coal play a key role in determining the methane adsorption capacity,[60,61] which provides an explanation for the close relationships between D_1 and desorption parameters A and V_1. In addition, the parameter K_t characterizes the ratio between the volume of the desorbed gas from the macropores and microfractures in the first minute after gas pressure is relieved and the total gas desorption volume.[62] Chen et al.[34] suggested that the methane desorption constant K_t is associated with the macropore volume. Obviously, for both dry coal and water-equilibrated coal, the constant K_t is closely related to D_2.

Moreover, many desorption parameters are applied to assess the risk of gas hazards in mining coal seams. For example, for the desorption indices Δh_2 and K_1, the outburst critical values for moist coal (Δh_2 = 160 Pa, K_1= 0.4 cm^3/(g·min$^{0.5}$)) are provided by industrial standards.[31,63,64] However, losses and fluctuations of adsorbed moisture in low-rank coal can affect the methane adsorption capacity of coal and sequentially lead to the variations in critical values of desorption indices for outburst prediction. It is necessary to study the quantitative relationships between methane desorption indices and moisture content and put forward a reasonable method for determining the critical values of methane desorption indices for in situ low-rank coal seams. Another revelation is that developing new engineering technologies to reduce the water content of low-rank coal is also necessary to improve gas migration in the development of coalbed methane (CBM).[22]

5. CONCLUSIONS

LN_2GA tests of the studied coal samples show that both N_2−SSA and N_2−PV decrease significantly along with the increases of moisture content, and the micropores with pore diameters less than 10 nm are most affected. In particular, when the moisture content of the coal sample increases to 10.88%, micropores with sizes less than 4 nm almost disappear in the DFT-PSDs, probably due to the blocking effects of water clusters and capillary water. However, the micropores (pore diameter <10 nm) still contribute most of the specific surface area for gas adsorption on the water-equilibrated coal even under the maximum relative humidity condition.

The fractal analyses of coal pores show that when the moisture content is less than 4.74%, D_1 decreases rapidly, whereas D_2 shows a slight reduction with the increases of moisture content, which is mainly due to the water adsorption on coal primarily occurring on the surfaces of micropores. However, when the moisture content exceeds 4.74%, D_2 decreases significantly, by contrast, nearly no change is observed for D_1 as the moisture content increases. These are most likely attributed to the completion of a monolayer for the adsorption of water molecules on micropores, and the pore-blocking effect of the adsorbed water in some pores and throats.

The water adsorbed by coal can reduce the gas desorption capacity of coal significantly, and each 1% increase in moisture content leads to an approximate 11% reduction in Q_1 and an approximate 8% reduction in Q_{3-5}. The correlation analyses between the desorption parameters and fractal dimensions indicate that the ultimate methane desorption capacity (A) and initial desorption rate (V_1) of coal are closely related to the fractal dimension D_1, while the desorption constant K_t of coal mainly depends on the fractal dimension D_2 under water-containing conditions.

AUTHOR INFORMATION

Corresponding Author

Mingyi Chen − *School of Safety Engineering and Emergency Management, Shijiazhuang Tiedao University, Shijiazhuang 050043, China; Hebei Province Technical Innovation Center of Safe and Effective Mining of Metal Mines, Shijiazhuang Tiedao University, Shijiazhuang 050043, China; Key Laboratory of Roads and Railway Engineering Safety Control, Shijiazhuang Tiedao University, Ministry of Education, Shijiazhuang 050043, China;* orcid.org/0000-0001-8384-2470; Email: chenmingyi@stdu.edu.cn

Authors

Xiaoyun Chen − *School of Safety Engineering and Emergency Management, Shijiazhuang Tiedao University, Shijiazhuang 050043, China*

https://doi.org/10.1021/acsomega.2c03805
ACS Omega 2022, 7, 37293−37303

Xuejie Zhang − *School of Safety Engineering and Emergency Management, Shijiazhuang Tiedao University, Shijiazhuang 050043, China; Key Laboratory of Roads and Railway Engineering Safety Control, Shijiazhuang Tiedao University, Ministry of Education, Shijiazhuang 050043, China*

Fuchao Tian − *State Key Laboratory of Coal Mine Safety Technology, China Coal Technology & Engineering Group, Shenyang Research Institute, Shenfu Demonstration Zone 113122, China;* orcid.org/0000-0002-7343-1448

Weili Sun − *State Key Laboratory of Coal Mine Safety Technology, China Coal Technology & Engineering Group, Shenyang Research Institute, Shenfu Demonstration Zone 113122, China*

Yumeng Yang − *School of Safety Engineering and Emergency Management, Shijiazhuang Tiedao University, Shijiazhuang 050043, China; Hebei Province Technical Innovation Center of Safe and Effective Mining of Metal Mines, Shijiazhuang Tiedao University, Shijiazhuang 050043, China; Key Laboratory of Roads and Railway Engineering Safety Control, Shijiazhuang Tiedao University, Ministry of Education, Shijiazhuang 050043, China*

Tonghao Zhang − *School of Safety Engineering and Emergency Management, Shijiazhuang Tiedao University, Shijiazhuang 050043, China*

Complete contact information is available at: https://pubs.acs.org/10.1021/acsomega.2c03805

Notes

The authors declare no competing financial interest.

■ ACKNOWLEDGMENTS

This work was financially supported by the National Natural Science Foundation of China (Grant Nos. 51804201, 52174230, and 51904272), the Natural Science Foundation of Hebei Province (Grant Nos. E2020210081 and E2021210128), and the University-Level Graduate Innovation Project (Grant No. YC2021029).

■ REFERENCES

(1) Busch, A.; Gensterblum, Y. CBM and CO2-ECBM related sorption processes in coal: a review. *International Journal of Coal Geology* **2011**, *87* (2), 49−71.

(2) Tahmasebi, A.; Yu, J. L.; Su, H. X.; Han, Y. N.; Lucas, J.; Zheng, H. L.; Wall, T. A differential scanning calorimetric (DSC) study on the characteristics and behavior of water in low-rank coals. *Fuel* **2014**, *135* (11), 243−252.

(3) Zhang, S.; Guo, W.; Li, Y. Experimental simulation of water-inrush disaster from the floor of mine and its mechanism investigation. *Arabian Journal of Geosciences* **2017**, *10* (22), 503.

(4) Pan, Z.; Connell, L. D.; Camilleri, M.; Connelly, L. Effects of matrix moisture on gas diffusion and flow in coal. *Fuel* **2010**, *89* (11), 3207−3217.

(5) Wang, C. Y.; Xing, Y. W.; Xia, Y. C.; Zhang, R.; Wang, S. W.; Shi, K. Y.; Tan, J. L.; Gui, X. H. Investigation of interactions between oxygen-containing groups and water molecules on coal surfaces using density functional theory. *Fuel* **2021**, *287*, 119556.

(6) Czerw, K.; Krzyzanowski, A.; Baran, P.Ł; Zarebska, K. Vapour sorption on coal: influence of polarity and rank. *Energies* **2022**, *15*, 3065.

(7) Chen, M. Y.; Cheng, Y. P.; Li, H. R.; Wang, L.; Jin, K.; Dong, J. Impact of inherent moisture on the methane adsorption characteristics of coals with various degrees of metamorphism. *Journal of Natural Gas Science & Engineering* **2018**, *55*, 312−320.

(8) Thararoop, P.; Karpyn, Z. T.; Ertekin, T. Numerical studies on the effects of water presence in the coal matrix and coal shrinkage and swelling phenomena on CO2-enhanced coalbed methane recovery process. *Int. J. Oil Gas Coal Technol.* **2012**, *5* (1), 47−65.

(9) Chang, Y.; Yao, Y.; Liu, D.; Liu, Y.; Cui, C.; Wu, H. Behavior and mechanism of water imbibition and its influence on gas permeability during hydro-fracturing of a coalbed methane reservoir. *J. Petrol. Sci. Eng.* **2022**, *208*, 109745.

(10) Goraya, N. S.; Rajpoot, N.; Sivagnanam, B. M. J. C. Coal bed methane enhancement techniques: a review. *Chemistry Select* **2019**, *4* (12), 3585−3601.

(11) Ojha, K.; Mandal, A.; Karmakar, B.; Pathak, A. K.; Singh, A. K. Studies on the Estimation and Prospective Recovery of Coal Bed Methane from Raniganj Coalfield, India. *ENERGY SOURCES PART A-RECOVERY UTILIZATION AND ENVIRONMENTAL EFFECTS* **2013**, *35*, 426−437.

(12) Ozdemir, E.; Schroeder, K. Effect of moisture on adsorption isotherms and adsorption capacities of CO_2 on coals. *Energy Fuels* **2009**, *23* (5), 2821−2831.

(13) Nie, B.; Liu, X.; Yuan, S.; Ge, B.; Jia, W.; Wang, C.; Chen, X. Sorption characteristics of methane among various rank coals: impact of moisture. *Adsorption* **2016**, *22* (3), 315−325.

(14) Gensterblum, Y.; Busch, A.; Krooss, B. M. Molecular concept and experimental evidence of competitive adsorption of H 2 O, CO 2 and CH 4 on organic material. *Fuel* **2014**, *115* (4), 581−588.

(15) Xiang, J. H.; Zeng, F. G.; Liang, H. Z.; Li, B.; Song, X. X. Molecular simulation of the $CH_4/CO_2/H_2O$ adsorption onto the molecular structure of coal. *Sci. China-Earth Sci.* **2014**, *57* (8), 1749−1759.

(16) Clarkson, C. R.; Bustin, R. M. Binary gas adsorption/desorption isotherms: effect of moisture and coal composition upon carbon dioxide selectivity over methane. *International Journal of Coal Geology* **2000**, *42* (4), 241−271.

(17) Laxminarayana, C.; Crosdale, P. J. Controls on Methane Sorption Capacity of Indian Coals. *AAPG Bulletin* **2002**, *86*, 201−212.

(18) Wang, F.; Yao, Y. B.; Wen, Z. A.; Sun, Q. P.; Yuan, X. H. Effect of water occurrences on methane adsorption capacity of coal: A comparison between bituminous coal and anthracite coal. *Fuel* **2020**, *266*, 117102.

(19) Meng, J. Q.; Li, S. C.; Niu, J. X.; Meng, H. X.; Zhong, R. Q.; Zhang, L. F.; Nie, B. S. Effects of moisture on methane desorption characteristics of the Zhaozhuang coal: experiment and molecular simulation. *Environ. Earth Sci.* **2020**, *79* (1), 44.

(20) Zhang, Z. G.; Cao, S. G.; Li, Y.; Guo, P.; Yang, H. Y.; Yang, T. Effect of moisture content on methane adsorption- and desorption-induced deformation of tectonically deformed coal. *Adsorpt. Sci. Technol.* **2018**, *36* (9−10), 1648−1668.

(21) Liu, Y. W.; Feng, G. Z.; Zuo, W. Q.; Liu, M. J.; Mitri, H. S. The law and mechanism of dynamic methane diffusion from coal particles under different moisture content. *Arabian Journal of Geosciences* **2019**, *12* (24), 748.

(22) Guo, H. J.; Yuan, L.; Cheng, Y. P.; Wang, K.; Xu, C.; Zhou, A. T.; Zang, J.; Liu, J. J. Effect of moisture on the desorption and unsteady-state diffusion properties of gas in low-rank coal. *Journal of Natural Gas Science and Engineering* **2018**, *57*, 45−51.

(23) Wang, L.; Chen, E.-t.; Liu, S.; Cheng, Y.-p.; Cheng, L.-b.; Chen, M.-y.; Guo, H.-j Experimental study on the effect of inherent moisture on hard coal adsorption-desorption characteristics. *Adsorpt.-J. Int. Adsorpt. Soc.* **2017**, *23* (5), 723−742.

(24) Wang, K.; Zang, J.; Feng, Y.; Wu, Y. Effects of moisture on diffusion kinetics in Chinese coals during methane desorption. *Journal of Natural Gas Science & Engineering* **2014**, *21* (2), 1005−1014.

(25) Wang, B. Y.; Yong, Q.; Jian, S.; Gang, W. Summarization of geological study on low rank coalbed methane in China. *Coal Science and Technology* **2017**, *45*, 170−190.

(26) Guo, H.; Cheng, Y.; Wang, L.; Lu, S.; Jin, K. Experimental study on the effect of moisture on low-rank coal adsorption characteristics. *Journal of Natural Gas Science & Engineering* **2015**, *24* (4), 245−251.

(27) Zou, L.; Gong, L.; Xu, P.; Feng, G.; Liu, H. Modified GAB model for correlating multilayer adsorption equilibrium data. *Separation & Purification Technology* **2016**, *161*, 38−43.
(28) Duan, S.; Li, G. D.Equilibrium and Kinetics of Water Vapor Adsorption on Shale. *Journal of Energy Resources Technology-Transactions of the ASME*2018, *140*(12), 122001.
(29) Andrade, R. D.; Lemus, R.; Perez, C. E. Models of Sorption Isotherms for Food: Uses and Limitations. *Vitae* **2011**, *18*, 325−334.
(30) Zhang, Y.*Geochemical kinetics*; Princeton University Press: Princeton, NJ, 2008.
(31) Cheng, Y. P.; Wang, H. F.; Wang, L.; Zhou, H. X.; Liu, H. B.; Wu, D. M.; Li, W.*Theories and Engineering Applications on Coal Mine Gas Control*; China University of Mining and Technology Press: Xuzhou, China, 2010.
(32) Airey, E. Gas emission from broken coal. An experimental and theoretical investigation. *International Journal of Rock Mechanics and Mining Sciences & Geomechanics Abstracts* **1968**, *5*, 475−494.
(33) Winter, K.; Janas, H.Gas emission characteristics of coal and methods of determining the desorbable gas content by means of desorbometers. *XIV International Conference of Coal Mine Safety Research*, 1975.
(34) Chen, M. Y.; Cheng, Y. P.; Zhou, H. X.; Wang, L.; Tian, F. C.; Jin, K. Effects of Igneous Intrusions on Coal Pore Structure, Methane Desorption and Diffusion within Coal, and Gas Occurrence. *Environmental & Engineering Geoscience* **2017**, *23* (3), 191−207.
(35) Banerjee, B. Spacing of fissuring network and rate of desorption of methane from coals. *Fuel* **1988**, *67* (11), 1584−1586.
(36) Lowell, S.; Shields, J. E.; Thomas, M. A.; Thommes, M.*Characterization of porous solids and powders: surface area, pore size and density*; Springer Science & Business Media: The Netherlands, 2004.
(37) Hong, L.; Gao, D. M.; Wang, J. R.; Zheng, D. The Power Source for Coal and Gas Outburst. *Journal of Mining Science* **2019**, *55* (2), 239−246.
(38) Kondo, S.; Ishikawa, T.; Abe, I.*Adsorption science*; Chemical Industry Press: Beijing, China, 2005.
(39) Thommes, M.; Kaneko, K.; Neimark, A. V.; Olivier, J. P.; Rodriguez-Reinoso, F.; Rouquerol, J.; Sing, K. S. Physisorption of gases, with special reference to the evaluation of surface area and pore size distribution (IUPAC Technical Report). *Pure Appl. Chem.* **2015**, *87* (9−10), 1051−1069.
(40) Liu, K. Q.; Zakharova, N.; Adeyilola, A.; Zeng, L. B. Experimental Study on the Pore Shape Damage of Shale Samples during the Crushing Process. *Energy Fuels* **2021**, *35* (3), 2183−2191.
(41) Qi, L. L.; Tang, X.; Wang, Z. F.; Peng, X. S. Pore characterization of different types of coal from coal and gas outburst disaster sites using low temperature nitrogen adsorption approach. *International Journal of Mining Science and Technology* **2017**, *27* (2), 371−377.
(42) Charrière, D.; Behra, P. Water sorption on coals. *J. Colloid Interface Sci.* **2010**, *344*, 460−467.
(43) Chen, Y.; Tang, D. Z.; Xu, H.; Tao, S.; Li, S.; Yang, G. H.; Yu, J. J. Pore and fracture characteristics of different rank coals in the eastern margin of the Ordos Basin, China. *Journal of Natural Gas Science and Engineering* **2015**, *26*, 1264−1277.
(44) Jiang, J.; Cheng, Y.; Mou, J.; Jin, K.; Cui, J. Effect of Water Invasion on Outburst Predictive Index of Low Rank Coals in Dalong Mine. *PLoS One* **2015**, *10* (7), e0132355.
(45) Gensterblum, Y.; Merkel, A.; Busch, A.; Krooss, B. M. High-pressure CH 4 and CO 2 sorption isotherms as a function of coal maturity and the influence of moisture. *International Journal of Coal Geology* **2013**, *118* (3), 45−57.
(46) Do, D. D.; Junpirom, S.; Do, H. D. A new adsorption-desorption model for water adsorption in activated carbon. *Carbon* **2009**, *47*, 1466−1473.
(47) Hazra, B.; Chandra, D.; Singh, A. K.; Varma, A. K.; Mani, D.; Singh, P. K.; Boral, P.; Buragohain, J. Comparative pore structural attributes and fractal dimensions of Lower Permian organic-matter-bearing sediments of two Indian basins: Inferences from nitrogen gas adsorption. *Energy Sources Part A-Recovery Util. Environ. Eff.* **2019**, *41* (24), 2975−2988.
(48) Liu, X. F.; Nie, B. S. Fractal characteristics of coal samples utilizing image analysis and gas adsorption. *Fuel* **2016**, *182*, 314−322.
(49) Li, Z.; Lin, B.; Gao, Y.; Cao, Z.; Cheng, Y.; Yu, J. Fractal analysis of pore characteristics and their impacts on methane adsorption of coals from Northern China. *International Journal of Oil, Gas and Coal Technology* **2015**, *10* (3), 306−324.
(50) Yao, Y.; Liu, D.; Tang, D.; Tang, S.; Huang, W. Fractal characterization of adsorption-pores of coals from North China: an investigation on CH 4 adsorption capacity of coals. *International Journal of Coal Geology* **2008**, *73* (1), 27−42.
(51) Hazra, B.; Wood, D. A.; Mani, D.; Singh, P. K.; Singh, A. K.Organic and Inorganic Porosity, and Controls of Hydrocarbon Storage in Shales. *Evaluation of Shale Source Rocks and Reservoirs*; Springer: Cham, Switzerland, 2019.
(52) Hazra, B.; Wood, D. A.; Singh, P. K.; Singh, A. K.; Kumar, O. P.; Raghuvanshi, G.; Singh, D. P.; Chakraborty, P.; Rao, P. S.; Mahanta, K.; et al. Source rock properties and pore structural framework of the gas-prone Lower Permian shales in the Jharia basin, India. *Arabian Journal of Geosciences* **2020**, *13* (13), 1−18.
(53) Hazra, B.; Vishal, V.; Singh, D. P. Applicability of Low-Pressure CO2 and N2 Adsorption in Determining Pore Attributes of Organic-Rich Shales and Coals. *Energy Fuels* **2021**, *35* (1), 456−464.
(54) Liu, S. L.; Zhang, D. F.; Lun, Z. M.; Zhao, C. P.; Wang, H. T. Occurrence of water within different rank coals: a review. *Energy Sources Part A-Recovery Util. Environ. Eff.* **2020**, DOI: 10.1080/15567036.2020.1781979.
(55) Švábová, M.; Weishauptová, Z.; Přibyl, O. Water vapour adsorption on coal. *Fuel* **2011**, *90* (5), 1892−1899.
(56) Wang, F.; Liang, Y.; Sun, Z.; Li, L.; Li, X. Determination of the sensitivity index and its critical value for outburst risk prediction: A case study in Fuxiang mine, China. *Adsorption Science and Technology* **2020**, *38*, 502.
(57) Liu, Y. W.; Zhang, J. Q.; Liu, M. J.; Ya-Peng, L. I. Influence of moisture content on gas diffusion coefficient of coal particles with different metamorphic degree. *J. Safety Sci. Technol.* **2015**, *11*, 12−17.
(58) Xu, H.; Tang, D. Z.; Zhao, J. L.; Li, S.; Tao, S. A new laboratory method for accurate measurement of the methane diffusion coefficient and its influencing factors in the coal matrix. *Fuel* **2015**, *158*, 239−247.
(59) Liu, P.; Liu, A.; Liu, S. M.; Qi, L. L. Experimental evaluation of ultrasound treatment induced pore structure and gas desorption behavior alterations of coal. *Fuel* **2022**, *307*, 121855.
(60) An, F. H.; Cheng, Y. P.; Wu, D. M.; Wang, L. The effect of small micropores on methane adsorption of coals from Northern China. *Adsorption* **2013**, *19* (1), 83−90.
(61) Song, D. Y.; Ji, X. F.; Li, Y. B.; Zhao, H. T.; Song, B. Y.; He, K. K. Heterogeneous development of micropores in medium-high rank coal and its relationship with adsorption capacity. *International Journal of Coal Geology* **2020**, *226*, 103497.
(62) Guo, J.; Kang, T.; Kang, J.; Zhao, G.; Huang, Z. Effect of the lump size on methane desorption from anthracite. *Journal of Natural Gas Science and Engineering* **2014**, *20*, 337−346.
(63) Cheng, L. B.; Wang, L.; Cheng, Y. P.; Jin, K.; Zhao, W.; Sun, L. S. Gas desorption index of drill cuttings affected by magmatic sills for predicting outbursts in coal seams. *Arabian Journal of Geosciences* **2016**, *9* (1), 61.
(64) Shu, L.; Wang, K.; Liu, Z.; Zhao, W.; Zhu, N.; Lei, Y. A Novel Physical Model of Coal and Gas Outbursts Mechanism: Insights into the Process and Initiation Criterion of Outbursts. *Fuel* **2022**, *323*, 124305.

https://doi.org/10.1021/acsomega.2c03805
ACS Omega 2022, 7, 37293−37303